Efficient hybrid eddy current simulation in thick cylinders and thin surfaces of arbitrary geometry induced by MRI gradient coils.

Hector Sanchez-Lopez[1], Michael Poole[1], Ewald Weber[1], Limei Liu[1], and Stuart Crozier[1]
[1]*ITEE, The University of Queensland, Brisbane, QLD, Australia*

Introduction: Eddy currents are one of the main causes of deleterious cross-talk within hybrid MRI scanners such as (IGRT-MRI) Image Guided Radiotherapy-MRI or PET-MRI systems. Currents induced in the conducting parts of scanners produce acoustic noise, power heating, magnetic field asymmetries and these undesired effects may cause unpleasant acoustic noise, electronic malfunctioning, frequency shift in the RF coil and imaging artifacts [1]. In this paper we present a new fast and efficient eddy current simulation method which combines current densities expressed as normalized Fourier series and linear basis functions. The hybrid approach is a combination of the network method [2] and boundary element method (BEM) for thin surfaces of arbitrary shape. The new method is capable of accurately simulating currents induced in thick cylinders of finite length (such as a cryostat) and thin surfaces of arbitrary shape by coils of arbitrary geometry. We present two examples to demonstrate the capabilities of the method in terms of predicting the induced currents, power losses, magnetic field harmonics and pre-emphasis simulations using arbitrary current pulse sequences.

Method: We define two conducting domains. In the first domain the current density is expressed as Fourier series and the conducting cylinder is divided into N layers of thickness h, where h is much smaller than the skin depth δ [2]. In the second domain (BEM) the current is expressed as linear basis functions [3] and the magnetic field, resistance and inductance are calculated in real space assuming a conducting surface thinner than the skin depth. The two conducting domains are inductively coupled but resistively decoupled. The boundary conditions and the edges of the domain are enforced to satisfy the continuity equation. The diffusion equation is solved for time-harmonic or transient solution when the coil is driven with an arbitrary current pulse [2].

In order to validate the results we assumed two conducting cylinders made of steel and copper. Two current loops are placed at z=±200 mm and driven by 2 A current at 1 kHz. The loops were set to a radius of 325.5 mm. The length, radius and thickness of the copper cylinder were set to 1 m, 300 mm and 1 mm, respectively. The length, radius, thickness and central gap of the steel cylinder were set to 1.3 m, 450 mm, 3 mm and 200 mm, respectively. The power was calculated using commercial software FEMLAB and the dependency of the number of nodes versus the average power loss was analyzed and compared with that produced by FEMLAB.

We simulated the currents induced in a simplified IGRT-MRI magnet where the cryostat is split in two halves. We assumed that the currents are mainly induced in the cylinders and much less significant in the cryostat ending disks. The central gap was 200 mm, the warm bore, cold shield and secondary cold shield lengths were 1.43 m, 1.4 m and 1.38 m, respectively. The thicknesses were set to 3 mm, 6 mm and 3 mm and the conductivities to $1.1\cdot10^6$ S/m, $3.8\cdot10^7$ S/m and $1.2\cdot10^9$ S/m. The conductivity in the 2 mm thick ellipsoids and the 2mm thick Gantry were set to $1.79\cdot10^7$ S/m and $1.1\cdot10^6$ S/m, respectively. 2208 triangles were used to discretize the BEM surfaces. The gradient coil was designed to generate 20 mT/m and the total magnetic energy was minimized while constraining the gradient of the secondary field produced by the eddy currents to be uniform in the region of interest of 20x20x20 cm. The primary and secondary coils were split (20 cm gap) and connected using a conical shape in order to minimize the inductive coupling between the connecting wires and the additional conducting structure inserted between the gradient coils. In the second example a copper RF shield of 12 ηm, 300 mm radius and 1 m axial length was simulated. The RF shield has 16 axial slits along the azimuthal direction. A similar strategy was used to design the gradient coil, but no gap was included. The primary and secondary coil radii were set to 344 mm and 435 mm, respectively and the axial length were set to 1.07 m and 1.36 m, respectively. The coils were designed using the equivalent magnetization current approach [4]. The results of the eddy current simulations were compared with that produced by the same model (cryostat and coil) but using a continuous RF shield.

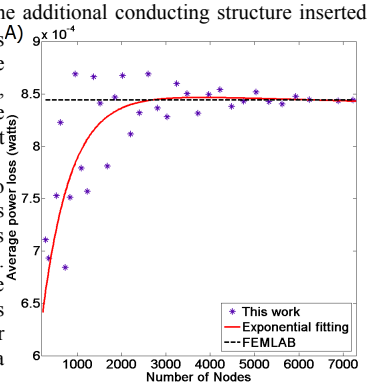

Results and Discussions: Figure (A) shows that, when the number of nodes increases, the average power loss tends to converge to the target value. This effect is due to the discrete nature of the BEM and the fact that the current density is approximated using linear basis functions. However, as the number of nodes increases, the computational time increases linearly. Figure (B) describes the currents induced in the split cryostat and in the BEM surfaces 1 and 2, respectively. High currents are induced in the BEM surfaces 1 (381 A) and the secondary cold shields (473 A); this is due to the proximity of surface 1 to the gradient coils and the poor shielding achieved due to the central gap. These currents produce 46 watts in the three ellipsoids and 22 watts in the secondary cold shield at 1 kHz. Figure (C) shows that, for frequencies larger than 2.5 kHz, BEM surface 2 generates more power losses than BEM 1. The BEM surfaces produce a significant contribution to spherical harmonics due to the eddy currents. Figure (D) shows the frequency response of some of the harmonics responsible for imaging artefacts. Within the range (1 kHz – 3.5 kHz), the BEM surfaces introduce a A_{00}=16 μT. The cryostat and the BEM surface produces an A_{11}=-73 μT of which -16μT are generated by the BEM surfaces. The cryostat produces an insignificant amount of zonal harmonics, however the BEM surfaces introduce A_{20}=-18 μT, A_{40}=-10.3 μT and A_{22}=4.5 μT, A_{31}=10 μT and A_{51}=-5 μT. The cryostat produces A_{22}=0.02 μT, A_{31}=0.8 μT and A_{51}=-0.01 μT, respectively. This is in accordance with the coil design strategy whereby the magnetic field was constrained to be as linear as the primary field; however this achievement is vitiated by the inclusion of the conducting parts. The simulation was obtained in 35 mins in an i7CPU at 2.8 GHz. The code was implemented in Matlab. Figures (E) and (F) show the current induced in the continuous and cut RF shield. In the cut RF shield the current induced is 4 times smaller than that produced by the continuous shield. About 30 times less accumulative power is generated by the cut RF shield as a consequence of the interruption of the flow of eddy currents on the RF shield surface (See Fig. G). In terms of field harmonics, the continuous RF shield produces a very high A_{11}=312μT which is generated only when the current is ramp-up and down. After that, the current in the RF shield completely decays and the cryostat generates A_{11}=94μT just after the current is ramp-up. This value is close to that generated by the cut RF shield and cryostat; even just 4.8μT larger than the value produced by the cryostat without an RF shield. This means that the cut RF shield is "transparent" to the gradient coils. In other words, the time rate at which a certain spatial magnetic field profile occurs is much smaller than the cryostat time decay constants. The cut RF shield has a decay constant in the range 1.1 μs to 15 μs while the cryostat has 44 μs to 0.93 s. This means that they never produce a time overlapping spatial magnetic field profile. Conversely, the continuous RF shield has a decay constant range of 2.3μs to 93.2 μs. This means that some spatial magnetic field profiles might be generated and superimposed in the common time range.

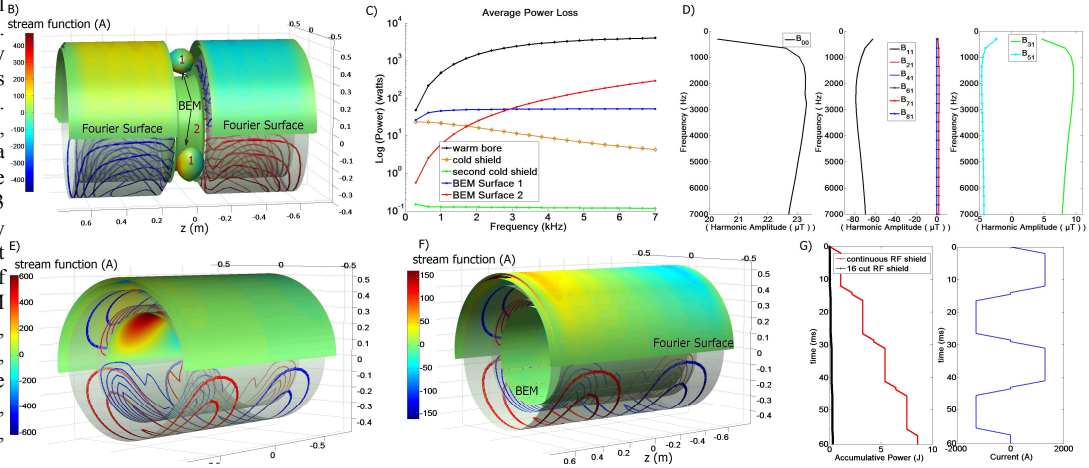

Conclusions: An efficient hybrid network method to simulate eddy currents induced by coils of arbitrary geometry in thick conducting cylinders and thin surfaces of arbitrary shape has been presented.

References: [1] C. S. Levin and H. Zaidi, *PET Clin,* vol. 2, pp. 125-160, 2007. [2] H Sanchez-Lopez *et al. Journal of Magnetic Resonance*, 207, 251-261, (2010). [3] S. Pissanetzky, *Meas. Sci. Technol.,* vol. 3, pp. 667-673, 1992. [4] H Sanchez-Lopez *et al Journal of Magnetic Resonance*, 199, 48-55, (2009).

Acknowledgements: This work was performed for MedTeQ, a Queensland Smart State funded research centre.